Z. WU*[)], H. JAKUBCZAK**[)], G. GLINKA*[)], K. MOLSKI***[)], L. NILSSON****[)]

DETERMINATION OF STRESS INTENSITY FACTORS FOR CRACKS IN COMPLEX STRESS FIELDS

Fatigue cracks in machine components are subjected to stress fields induced by the external load and residual stresses resulting from the surface treatment. Stress fields in such cases are characterized by non-uniform distributions and handbook stress intensity factor solutions for such configurations are not available. The method presented below is based on the generalized weight function technique enabling the stress intensity factors to be calculated for any Mode I loading applied to arbitrary planar convex crack. The method is particularly suitable for modeling fatigue crack growth in presence of complex stress fields.

1. Introduction

Fatigue durability, damage tolerance and strength evaluation of notched and cracked structural members require calculation of stress intensity factors for cracks located in regions characterized by complex stress fields. This is particularly true for cracks emanating form notches or other stress concentration regions that are frequently found in mechanical and structural components. In the case of engine components, complex stress distributions are often due to temperature, geometry and surface finish resulting in

*[)]   *Department of Mechanical Engineering, University of Waterloo, Waterloo, Ontario N2L 3G1, Canada; E-mail: gggreg@mecheng1.uwaterloo.ca*

**[)]   *Warsaw Univ. of Technology, Inst. of Construction Machinery Engineering, Narbutta 84, 02-524 Warsaw, Poland; E-mail: Hieronim.Jakubczak@simr.pw.edu.pl*

***[)]   *Bialystok Technical University, Wiejska 45c, 15-351 Bialystok, Poland; E-mail: kmolski@pb.bialystok.pl*

****[)] *SAQ KONTROLL AB, Box 49306, 100 29 Stockholm, Sweden; E-mail: gggreg@mecheng1.uwaterloo.ca*

superposition of applied mechanical, thermal and residual stresses. In the caseof welded or riveted structural components, it is often necessary to deal with cracked components repaired by overlapping patches. Such components require fatigue analysis of a crack or cracks propagating through a variety of interacting stress fields. Moreover, these are often planar two-dimensional surface or buried cracks with irregular shapes. The existing handbook stress intensity factor solutions are not sufficient in such cases due to the fact that most of them have been derived for simple geometry and load configurations. The variety of notch and crack configurations, and the complexity of stress fields occurring in engineering components require more versatile tools for calculating stress intensity factors than the currently available ready made solutions, obtained for a range of specific geometry and load combinations.
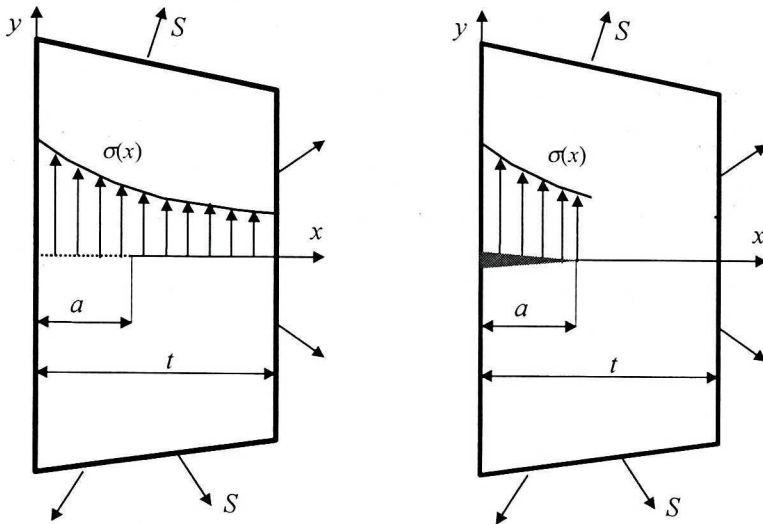

Fig. 1. The concept of superposition: (a) applied reference stress system and the corresponding local stress distribution $\sigma(x)$ in the prospective crack plane; (b) the local stress system $\sigma(x)$

Therefore, a method for calculating stress intensity factors for one- and two-dimensional cracks subjected to arbitrary stress fields is discussed below. The method is based on the use of the weight function technique. The weight function method developed by Bueckner [1] and Rice [2], and a variety of weight functions have been derived and published [7], [8], [9], [10] already. The important feature of a weight function is that it depends only on the geometry of the cracked body. If the weight function is known for a cracked body, the stress intensity factor due to any Mode I load system applied to the body can be determined by using this weight function. The success of the

weight function technique for calculating stress intensity factors lies in the possibility of using superposition. It can be shown, [17], that the stress intensity factor for a cracked body (Fig. 1) subjected to the external loading, S, is the same as the stress intensity factor in a geometrically identical body with the local stress field $\sigma(x)$ applied to the crack faces. The local stress field, $\sigma(x)$, induced in the prospective crack plane by the external load, S, is determined for uncracked body, which makes the stress analysis relatively simple.

If the weight function is known there is no need to derive ready-made stress intensity factor expressions for each load system and associated internal stress distribution induced in the cracked body. The stress intensity factor for a one-dimensional crack (Fig. 1) can be obtained by multiplying the weight function, $m(x, a)$, and the internal stress distribution, $\sigma(x)$, in the prospective crack plane, and integrating the product over the crack length a.

$$K = \int_0^a \sigma(x) \cdot m(x, a)\, dx \tag{1}$$

2. Weight functions for one-dimensional cracks

A variety of one-dimensional (line load) weight functions can be found in Refs [3], [4], [5], [6]. However, their mathematical forms vary from case to case making their application inconvenient. Therefore Glinka and Shen [7] have proposed a general expression (2) for a variety of weight functions corresponding to one-dimensional Mode I cracks.

$$m(x, a) = \frac{2}{\sqrt{2\pi(a - x)}} \left[1 + M_1 \left(1 - \frac{x}{a} \right)^{\frac{1}{2}} + M_2 \left(1 - \frac{x}{a} \right)^1 + M_3 \left(1 - \frac{x}{a} \right)^{\frac{3}{2}} \right] \tag{2}$$

The system of coordinates and notation for an edge crack as an example are given in Fig. 2. In order to determine the weight function, $m(x, a)$, for a particular cracked body, it is sufficient to determine the three parameters M_1, M_2 and M_3.

Because the mathematical form of the weight function (2) is the same for all cracks, the same method can be used for the determination of parameters M_i and calculation of stress intensity factors based on Eq. (1). The method of finding M_i parameters was discussed in reference [8]. The parameters can be determined from Eq. (1), providing that three reference stress intensity factor expressions K_{r1}, K_{r2} and K_{r3}, corresponding to three different stress distributions $\sigma_1(x)$, $\sigma_2(x)$ and $\sigma_3(x)$ respectively are known. The stress

distribution expressions and the general weight function of Eq. (2) can be substituted for $\sigma(x)$ and $m(x, a)$ in Eq. (1) resulting in three simultaneous equations, sufficient for the determination of the three unknown parameters M_1, M_2 and M_3.
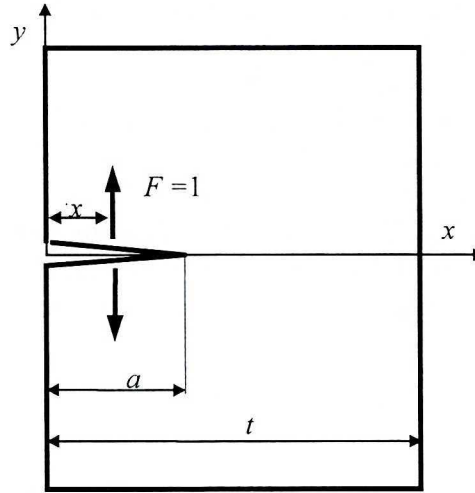

Fig. 2. Weight function for one-dimensional edge crack in a finite width plate; nomenclature

A possibility of reducing the number of reference SIFs by one comes from the property of weight functions. The third condition, necessary to determine parameters M_1, M_2 and M_3 can be formulated from the knowledge of the crack surface curvature at the crack mouth (free corner). Fett [16] showed that at x = 0 (Fig. 2) the curvature of an edge crack in the x-y plane should reduce to zero. Taking into account the relation between the weight function $m(x, a)$ and the crack opening displacement field derived by Bueckner [1] and Rice [2], it can be shown that the second derivative of the weight function at $x = 0$ must also be zero, i.e.

$$\frac{\partial^2 m(x, a)}{\partial x^2}\bigg|_{x=0} = 0 \tag{3}$$

It can be subsequently shown that Eq. (2) associated with expression (3) results in a constant value of the parameter $M_2 = 3$ regardless of the crack geometry. Therefore only two reference stress intensity factors are necessary for the determination of the two remaining parameters M_1 and M_3. Weight functions for an edge and central trough cracks in plate are enclosed in the
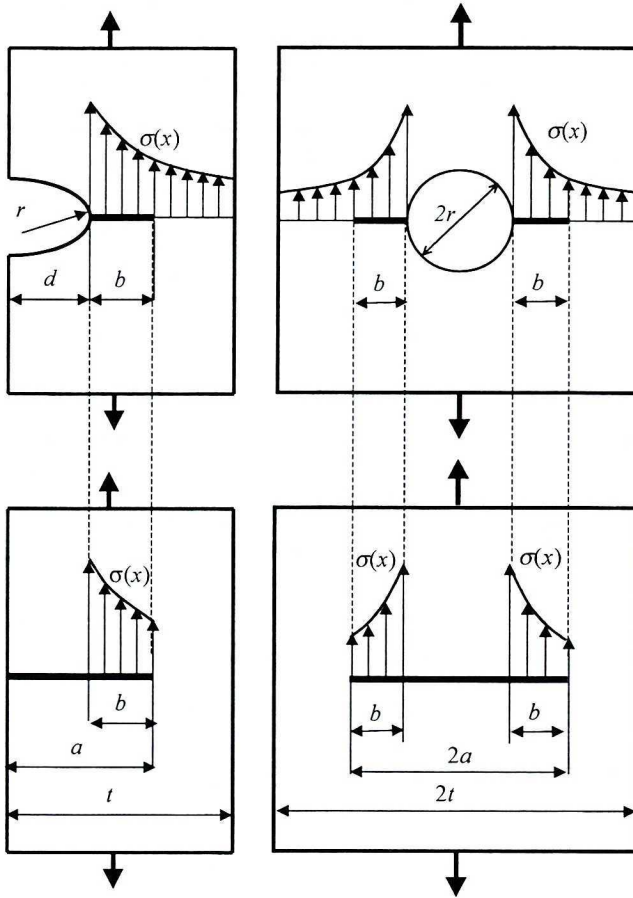
Appendix.

Fig. 3. Models for calculation of stress intensity factor for cracks emanating from notches

The weight functions can be used for calculation of stress intensity factors for cracks emanating from notches. In such cases the crack is modeled according to Fig. 3, i.e. the notch depth, r, is added to the actual crack length.

Results presented in Figures 4 and 5 in terms of the geometrical correction factor, Y, ($Y = \dfrac{K}{S\sqrt{\pi a}}$, where S is the remote stress) show a fairly good agreement of SIFs calculated using the weight function with those calculated by FEM.
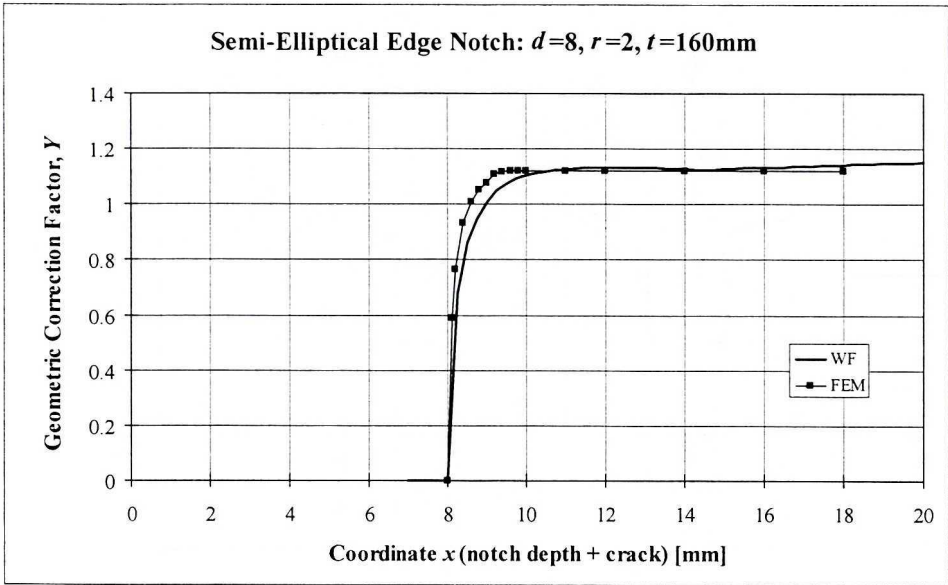
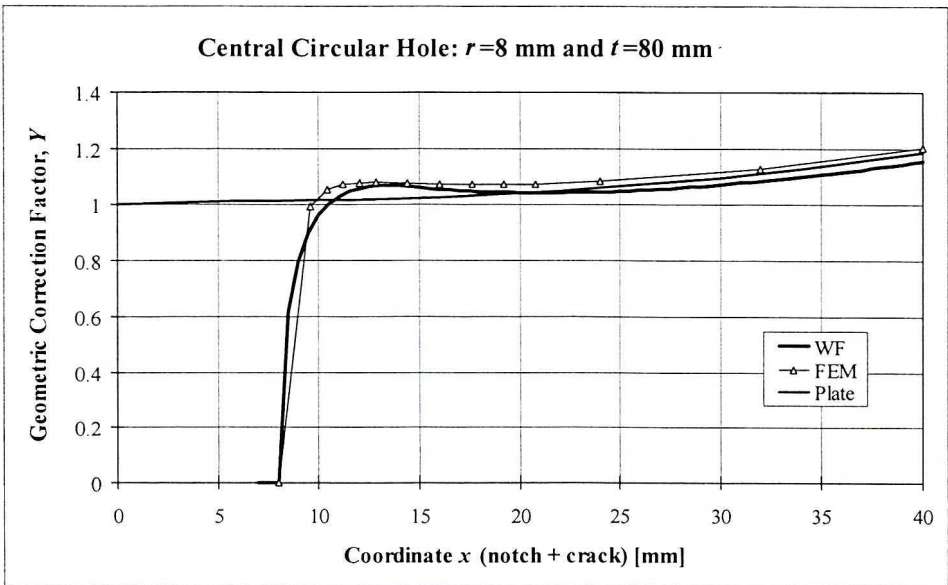Fig. 4. Comparison of the weight function based SIFs with FEM data for crack emanating from an edge notch

Fig. 5. Comparison of the weight function based SIFs with FEM data for crack emanating from a central circular hole

3. Line load weight functions for planar cracks subjected to one-dimensional stress fields

Fatigue and fracture analysis of cracked bodies often requires the calculation of SIF for embedded and surface semi-elliptical cracks. Stress intensity factors for surface semi-elliptical cracks are known only for a few simple load cases, i.e. Newman-Raju [18] solutions for pure tension and bending and Shiratori et al. [19] solutions for three exponential stress distributions. For more complex stress distributions the possibility of calculating SIF offers the weight function method.

Shen and Glinka [9] have found that the weight function for the deepest point, A, of a semi-elliptical crack (Fig. 6) in a one-dimensional non-uniform stress field $\sigma(x)$ can be approximated by Eq. (4), which is similar to Eq. (2). An analogous Eq. (5) can be used to approximate the weight function for the point B in the boundary layer near the surface of semi-elliptical crack in a flat plate.

$$m_A(x, a, a/c, a/t) = \frac{2}{\sqrt{2\pi(a-x)}} \left[1 + M_{1A}\left(1 - \frac{x}{a}\right)^{\frac{1}{2}} + M_{2A}\left(1 - \frac{x}{a}\right)^1 + \right.$$

$$\left. + M_{3A}\left(1 - \frac{x}{a}\right)^{\frac{3}{2}} \right] \tag{4}$$

$$m_B(x, a, a/c, a/t) = \frac{2}{\sqrt{\pi x}} \left[1 + M_{1B}\left(\frac{x}{a}\right)^{\frac{1}{2}} + M_{2B}\left(\frac{x}{a}\right)^1 + M_{3B}\left(\frac{x}{a}\right)^{\frac{3}{2}} \right] \tag{5}$$

The derivation of these two weight functions can be reduced to determination of parameters M_{1A}, M_{2A} and M_{3A} and M_{1B}, M_{2B} and M_{3B} respectively. The method of three reference SIFs discussed above for one-dimensional cracks can be used for that purpose.

The method of two reference SIFs, discussed earlier, can also be used for determination of parameters M_{1A} and M_{3A} for the deepest point. The parameter M_{2A} is calculated from the Eq. (2), thus it is the same as for one-dimensional cracks, i.e. $M_{2A} = 3$. The third condition necessary for determination of parameters M_{1B}, M_{2B} and M_{3B} was derived by satisfying the requirement that the weight function (5) must vanish

for $x = a$, i.e. $m_B(a, x, a/c, a/t) = 0$. Thus, the third equation can be written in the following form:

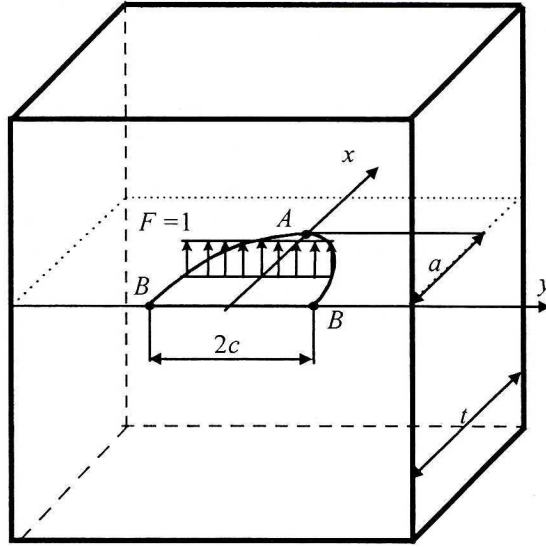$$1 + M_{1B} + M_{2B} + M_{3B} = 0 \qquad (6)$$

Fig. 6. Semi-elliptical surface crack under the unit line load;
The geometrical configuration and the line load weight function notation

In order to determine the SIF K_A and K_B induced by one-dimensional stress field, $\sigma(x)$, at points A and B, respectively, the product of the stress field, $\sigma(x)$, and the weight function, $m_A(x, a, a/c, a/t)$ and $m_B(x, a, a/c, a/t)$, needs to be integrated over the entire crack depth a, according to expression (1).

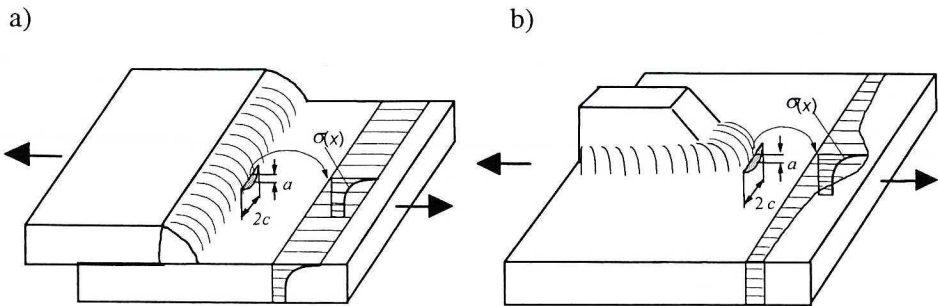a)   b)

Fig. 7. Stress distribution in the plane of a surface crack emanating from the weld toe

The one-dimensional line load weight functions are very efficient and useful if the stress distribution changes along the x coordinate only (Fig. 7a). However, they cannot be used if the stress field is two-dimensional in nature, i.e., when the stress field, $\sigma(x, y)$, in the crack plane depends on both x and y coordinates (Fig. 7b). Therefore, in order to calculate stress intensity factors for planar cracks subjected to two-dimensional stress fields a weight function for a point load is needed.

4. Point load weight functions for planar cracks subjected to two-dimensional stress fields

The two-dimensional point-load weight function, $m_A(x, y)$, represents the stress intensity factor at point A on the crack front, induced by a pair of unit forces, F, applied to the crack surface at point $P(x, y)$ (Fig. 8). If such a weight function is known, it is possible to calculate the stress intensity factor at any point on the crack front induced by any Mode I stress fields applied to the crack surface. In order to determine the SIF induced by a two-dimensional stress field, $\sigma(x, y)$, at the point A on the crack front, the product of the stress field, $\sigma(x, y)$, and the weight function, $m_A(x, y)$, needs to be integrated over the entire crack surface area, Ω.

$$K_A = \iint_{\Omega} \sigma(x, y) \, m_A(x, y; F) \, dxdy \tag{7}$$

Rice has shown [11] that the 2-D point load weight function for an arbitrary planar crack in an infinite body can be generally written as:

$$K_A = m_A(x, y; F) = \frac{F\sqrt{2\,s}}{\pi^{3/2}\rho^2} w_A(x, y; F) \tag{8}$$

Oore and Burns [12] proposed an approximate 2-D point-load weight function (9), from which the function $w(x, y; F)$ can be derived for a number of crack configurations.

$$K_A = m_A(x, y; F) = \frac{F\sqrt{2}}{\pi\rho^2 \sqrt{\int_{G_c} \dfrac{dG_c}{\rho_i^2}}} \tag{9}$$

The notation for the weight functions (8) and (9) is given in Figure 8, where ρ is the distance from the point load F to point A on the crack front, and

s is the shortest distance from the point load *F* to the crack front. Oore and Burns [12] have shown that after deriving closed form expressions for the line integral in expression (9), several exact weight functions could be derived for straight and circular cracks in infinite bodies.
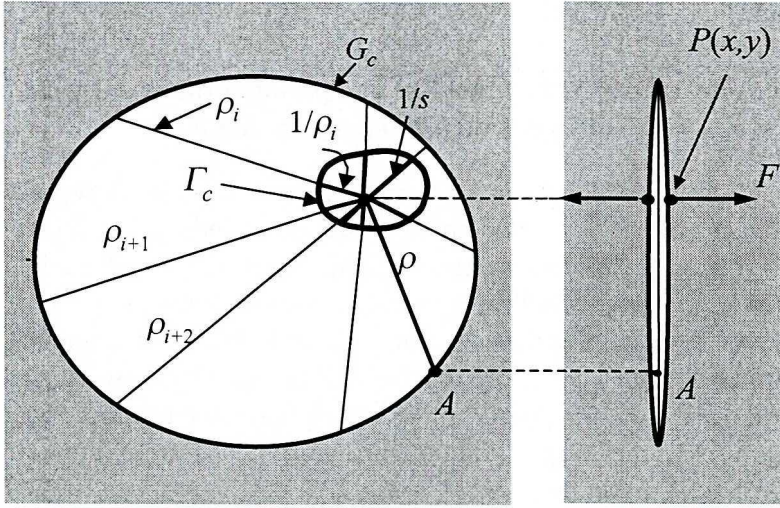

Fig. 8. Point load (2-D) weight function notation

It can also be proved that the line integral represents the arc length, Γ_c, of the crack contour inverted (Fig. 8) with respect to the point, $P(x, y)$. As a consequence the weight function, Equation (9), can be written in a shorter form.

$$K_A = m_A(x, y; F) = \frac{F\sqrt{2}}{\pi \rho^2 \sqrt{\Gamma_c}} \qquad (10)$$

The inverted contour, Γ_c, can be also looked at (Fig. 8) as the locus of inverted radii $1/\rho_i$. It can also be proved that inverted contours form circles in the case of straight and circular crack contours. In other words, the inverted contour is a circle in the case of cracks with a constant curvature. Subsequently, the weight function (10) makes it possible to derive closed form weight functions for a variety of straight and circular crack configurations.

4.1. Point load weight functions for planar cracks in infinite bodies

Based on eq.(10) Glinka and Reinhardt [13] have derived several point load weight functions for planar cracks in infinite bodies listed below.

The point load weight function for an infinite edge crack in an infinite body (Fig.9a):

$$K_A = m_A(x, y; F) = \frac{F\sqrt{s}}{\pi^{3/2}\rho^2}\sqrt{2} \tag{11}$$

Point load weight function for an infinite tunnel crack of width $2a$ (Fig. 9b) in an infinite body:

$$K_A = m_A(x, y; F) = \frac{F\sqrt{s}}{\pi^{3/2}\rho^2}\sqrt{2 - \frac{s}{a}} \tag{12}$$
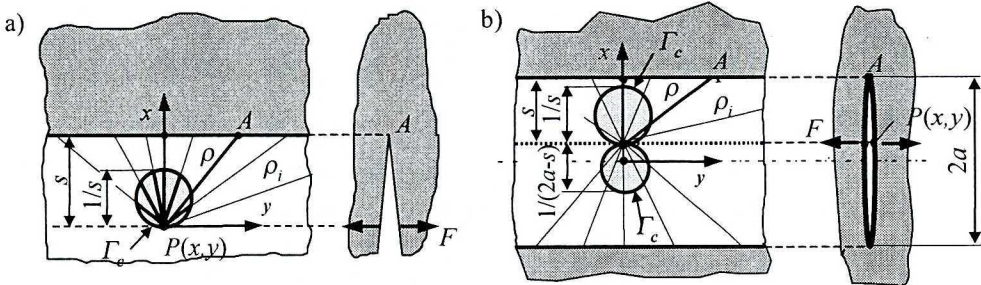

Fig. 9. An infinite edge crack (a) and a tunnel crack (b)

Line load weight function for an infinite tunnel crack of constant width $2a$ in an infinite body is:

$$K_A = m_A(x; F) = \int_{x=a-s} \frac{F\sqrt{s}}{\pi^{3/2}\rho^2}\sqrt{2 - \frac{s}{a}}\, dy = \frac{F\sqrt{2}}{\sqrt{\pi s}}\sqrt{\frac{2a - s}{2a}} \tag{13}$$

Weight function (13) is the well-known line load weight function for a through crack in an infinite plate derived by Sih [20]. Because the weight function (13) was derived from the general weight function (12), it indicates that expression (9) correctly accounts for all important effects of geometry and loading.

4.2. Embedded cracks in finite bodies the external boundary effect

The point load weight functions derived above indicate that the general weight function (10) may supply accurate SIF results for cracks in infinite bodies. However, in the case of finite bodies both the crack contour and the free boundary contour have to be considered. By analyzing the structure of existing point load functions it was found that the point load weight function (14) accounts well for the free boundary effect.

$$K_A = m_A(x, y; F) = \frac{F\sqrt{2}}{\pi \rho^2} \cdot \frac{\sqrt{\Gamma_c + \Gamma_b}}{\Gamma_c} \tag{14}$$

The weight function (14) was subsequently used to derive a few specific weight functions for crack configurations available in the literature such as:

● *An infinite straight edge crack approaching a straight free boundary* (Fig. 10a):

$$K_A = m_A(x, y; F) = \frac{F\sqrt{2s}}{\pi^{3/2}\rho^2}\sqrt{1 + \frac{s}{d}} \tag{15}$$

The point load weight function (15) can be further integrated along the line $x = 0$ resulting in the 1-D line load weight function (16) for an edge crack approaching a free straight boundary (without bending or rotation).

$$K_A = m_A(s; F) = \int_{x=0} \frac{F\sqrt{2s}}{\pi^{3/2}\rho^2}\sqrt{1 + \frac{s}{d}}\, dy = \frac{F\sqrt{2}}{\sqrt{\pi s}}\sqrt{1 + \frac{s}{d}} \tag{16}$$
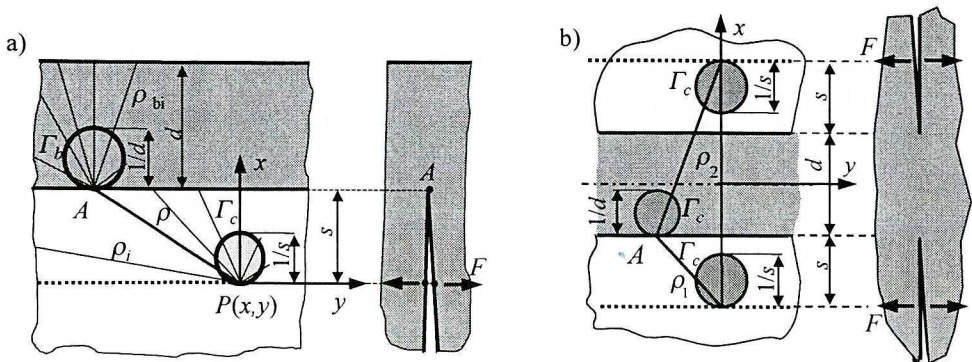

Fig. 10. An infinite crack approaching free boundary (a) and two infinite symmetric edge cracks separated by finite thickness ligament d (b)

- *Two infinite edge cracks under symmetric loading and separated by a ligament d* (Fig. 10b):

$$K_A = m_A(s, d; F) = \left(\frac{F\sqrt{2}}{\pi \rho_1^2} + \frac{F\sqrt{2}}{\pi \rho_2^2} \right) \cdot \frac{\sqrt{\Gamma_c + \Gamma_b}}{\Gamma_c} = \frac{F\sqrt{2s}}{\pi^{3/2}} \sqrt{\frac{d + s}{d}} \left(\frac{1}{\rho_1^2} + \frac{1}{\rho_2^2} \right) \quad (17)$$

Integration of the point load weight function (17) along the two lines of $x = 6(d/2 + s)$ for an uniformly distributed line load F resulted in the well-known [21] line weight function (18).

$$K_A = m_A(x, y; F) = \frac{F\sqrt{2}}{\sqrt{\pi s}} \frac{d + 2s}{\sqrt{d(d+s)}} \sqrt{1 + \frac{s}{d}} \quad (18)$$

4.3. Point load weight function of edge crack in finite bodies

The weight function (18) is valid for two infinite edge cracks separated by a finite ligament. When the crack depth is finite the crack mouth boundary effect has to be taken into account. Again, the general weight function (14) was also used to derive the point load weight function (19) for symmetrically loaded two finite edge cracks separated by a ligament of finite thickness $2d$ (Fig. 11a). The weight function (19) consists of two terms. The first part represents the contribution from the pure tension induced by the force F while the second term accounts for the finite crack depth. The crack mouth can be considered to be a symmetry line for an imaginary symmetric load.
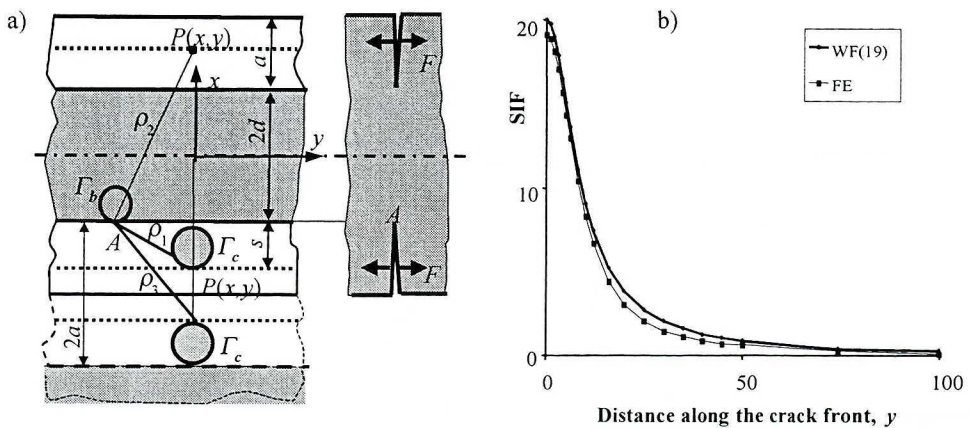

Fig. 11. Double edge crack in a finite body: (a) notations and (b) comparison with Tada's solution ($a/w = 0.5$; $a = 10$, $d = 10$, $s = 7.6563$).

$$K_A = m_A(x, y; F) = \left(\frac{F\sqrt{2}}{\pi \rho_1^2} + \frac{F\sqrt{2}}{\pi \rho_2^2} \right) \cdot \frac{\sqrt{\Gamma_c + \Gamma_b}}{\Gamma_c} + \frac{F\sqrt{2}}{\pi \rho_3^2 \sqrt{\Gamma_c}} \qquad (19)$$

Integration of equation (19) along the line $x = s$ resulted in the derivation of the line load weight function (20) for double edge crack (Fig. 11a) which agrees well with Tada's [211] solution (see Fig. 11b)

$$K_A = m_A(s; F) = \frac{2F}{\sqrt{\pi d s}} \frac{d + s}{\sqrt{s + 2d}} + \frac{\sqrt{2F}}{\sqrt{\pi}} \frac{\sqrt{s}}{2a - s} \qquad (20)$$

4.4. Point load weight function for a single edge crack

The weight function (21) for the crack configuration shown in Fig. 12a can be derived from general weight function (18). The difference between the single edge crack and symmetrically loaded double edge crack is that the single edge cracked body will bend under the point load F. Therefore the bending moment contribution has been added to the weight function (19).

$$K_A = m_A(x, y; F) = \left(\frac{F\sqrt{2}}{\pi \rho_2^2} + \frac{F\sqrt{2}}{\pi \rho_2^2} \right) \cdot \frac{\sqrt{\Gamma_c + \Gamma_b}}{\Gamma_c} + \frac{F\sqrt{2}}{\pi \rho_3^2 \sqrt{\Gamma_c}} +$$

$$+ 3 \cdot 975 \frac{F \sqrt{\left(s + \frac{d}{2} \right)^2 - \left(\frac{d}{2} \right)^2}}{d^{3/2}} \qquad (21)$$
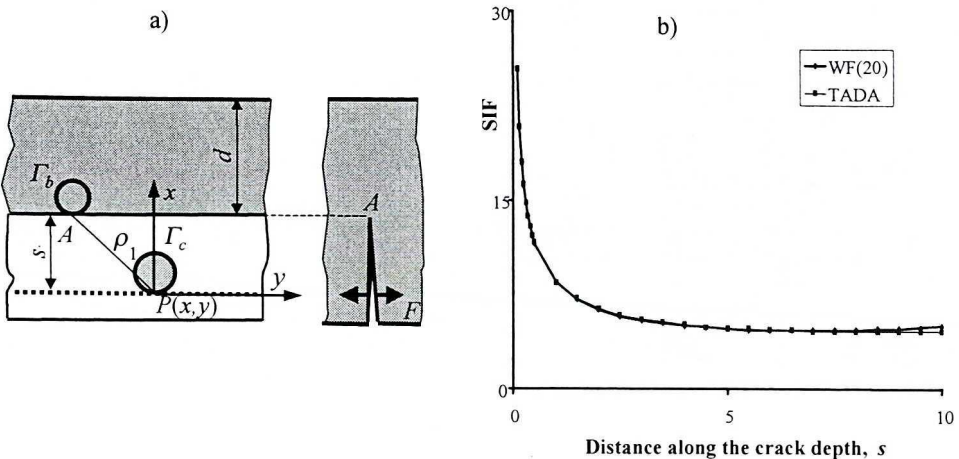

Fig. 12. An edge crack: (a) notation, and (b) the comparison of Eq. 20 with Tada's [211] solution

The weight function was also in good agreement with in house generated FEM results obtained for the same crack configuration (Fig. 12b).

4.5. Planar cracks with variable crack front curvature – the local curvature effect

It was also found that the accuracy of the weight function (14) and the subsequent accuracy of stress intensity factors for elliptical cracks, was decreasing as the ellipses became more slender, i.e., when they departed significantly from the circular constant curvature contour. It was concluded that the inverted crack contour, Γ_c in equation (10), is only an average measure of the crack geometry effect. The weight function and the stress intensity factor depend also on the immediate curvature surrounding the point where the stress intensity factor is to be calculated (Fig. 13). The correction for the local curvature effect proposed below is empirical in nature and was deducted from the stress intensity data for a wide variety of SIFs for semi-elliptical surface cracks and properties of weight functions.

$$K_A = m_A(x, y; F) = \left(\frac{F\sqrt{2}}{\pi \rho_1^2} + \frac{F\sqrt{2}}{\pi \rho_2^2} \right) \cdot \frac{\sqrt{\Gamma_b + \Gamma_c \left(\dfrac{a}{r_A} \right)^{1/2}}}{\Gamma_c \left(\dfrac{a}{r_A} \right)^{1/2}} + \frac{F}{\pi \rho_3^2 \sqrt{\Gamma_c \left(\dfrac{a}{r_A} \right)^{1/2}}} \quad (22)$$

- *Stress intensity factors for a pair of semi-elliptical surface cracks in a finite thickness plate*
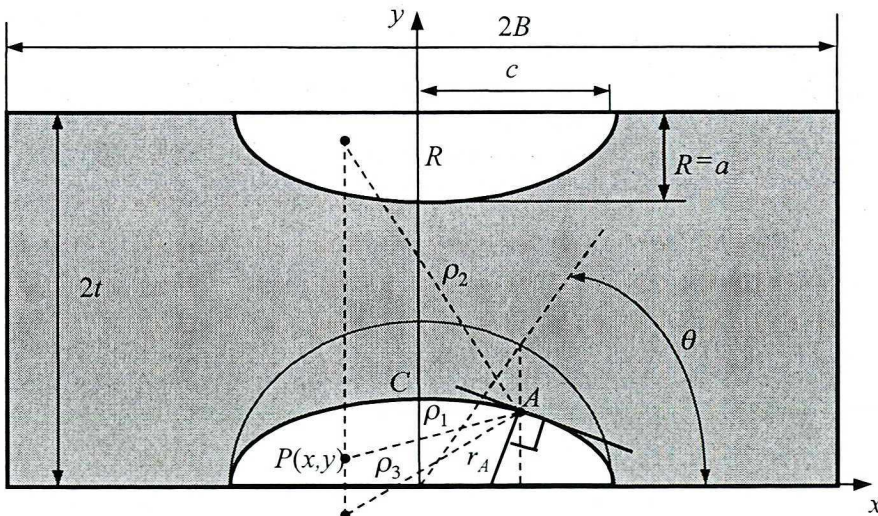

Fig. 13. A finite thickness plate with a pair of symmetric semi-elliptical surface cracks

Using the point load weight function (14), one can determine the stress intensity factor K for a pair of symmetric semi-elliptical cracks in a finite thickness plate (Fig. 13).

The stress intensity factors at the deepest point C (Fig. 13) were determined for a uniform tensile stress field, $\sigma(x, y) = \sigma_0 = 1$ using numerical integration of the weight function (22). The comparison of calculated SIFs in terms of the geometric correction factor, $Y = \dfrac{K}{\sigma_0 \cdot \sqrt{\pi a}}$, with Isida et. al [14] data is presented (Fig. 14) for cracks with relative depth of $a/t = 0.5$. For the relative crack depths within the range of $0.2 < a/t < 0.8$, the maximum difference between those two sets of data was 7.9%.

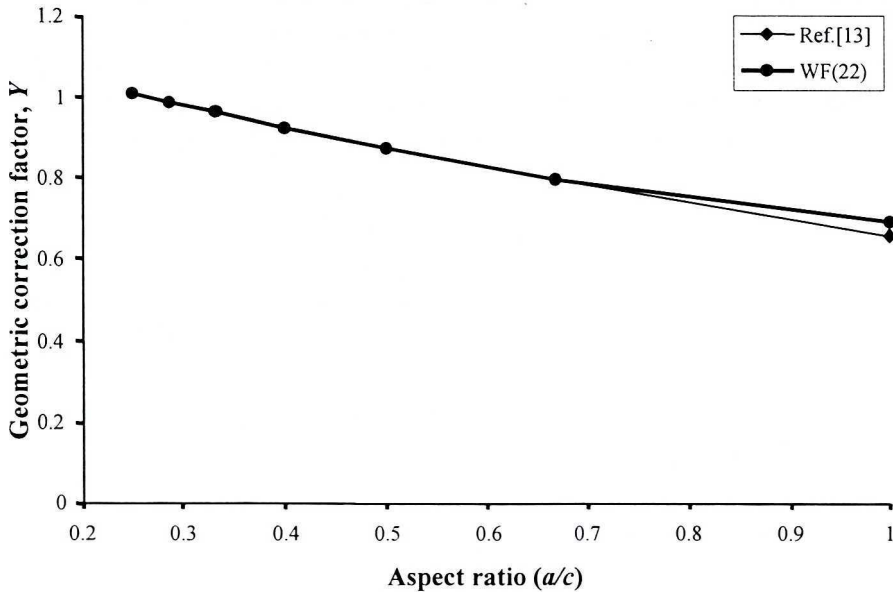
Fig. 14. Comparison of the weight function based SIFs with Isida, et. al data for various aspect ratios a/c and the relative depth $a/t = 0.5$

- *Stress intensity factors for a semi-elliptical surface crack in a finite thickness plate*

The notation for a semi-elliptical surface crack in a finite thickness plate is shown in Figure 15. The weight function (22) was used for the determination of the SIF for this crack configuration.

Two virtual symmetric loads were used to account for the free boundary and the crack mouth effect. The weight function (22) gave good SIF estimations for semi-circular surface crack ($a/c = 1$) with relative depth of

$0 < a/t \le 0.8$. The error was less than a few percent for two non-uniform stress fields used for comparisons, i.e. $\sigma(x, y) = \sigma_0 * x/c$ and $\sigma(x, y) = \sigma_0 * xy/ac$. The stress field $\sigma(x, y) = \sigma_0 * xy/a$ is shown graphically in Fig. 16.
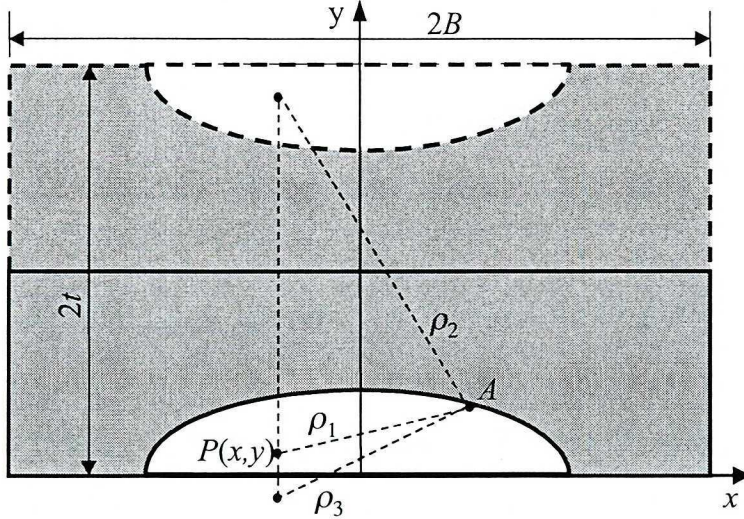

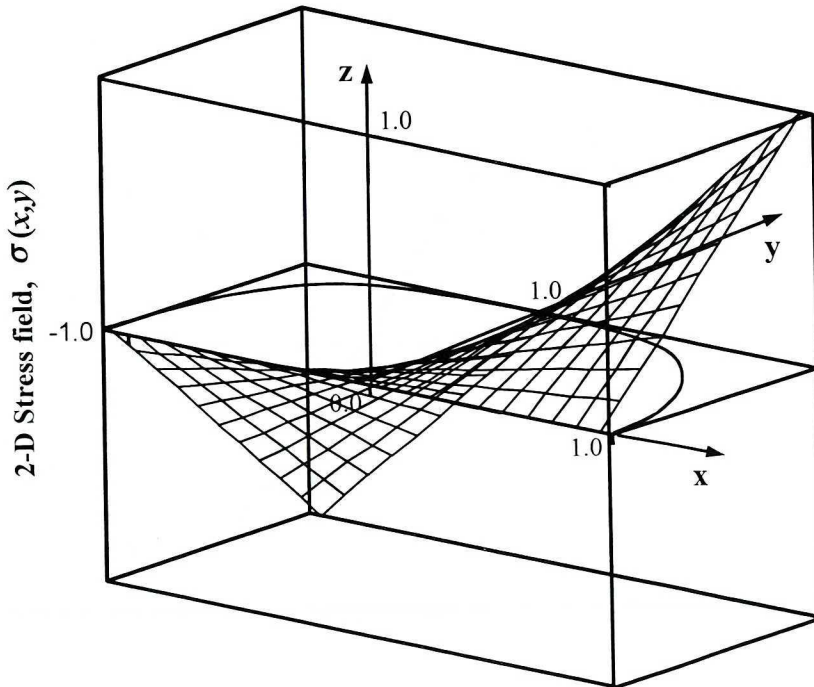Fig. 15. Semi-elliptical surface crack in a finite thickness plate

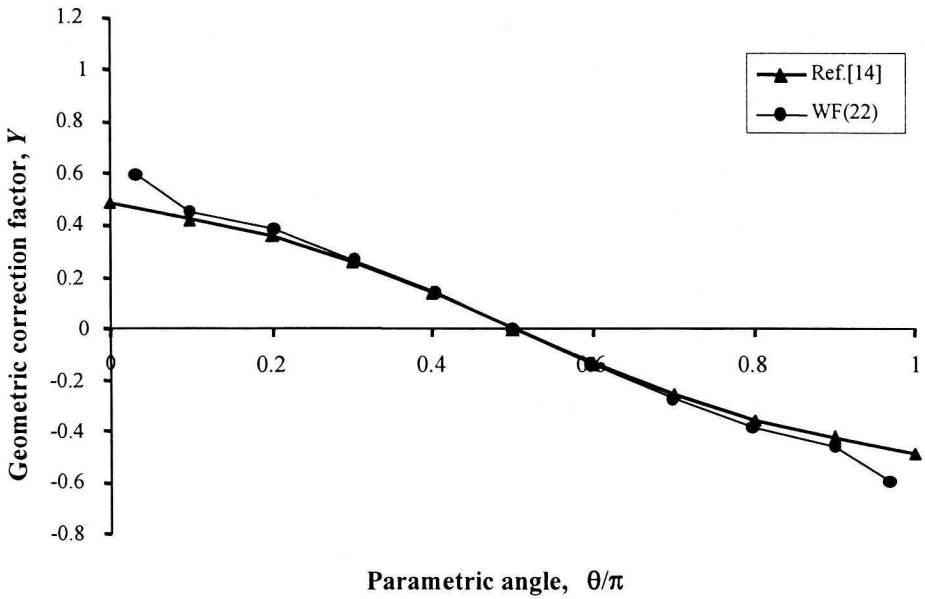Fig. 16. Two-Dimensional stress field, $\sigma(x, y) = \sigma_0 * xy/ac$ applied to the crack surface

Fig. 17. (a) Comparison of the weight function based geometric correction factor Y with Nilsson's [15] FE data, $[\sigma(x, y) = \sigma_0 * x/c, a/c = 1, a/t = 0.8]$
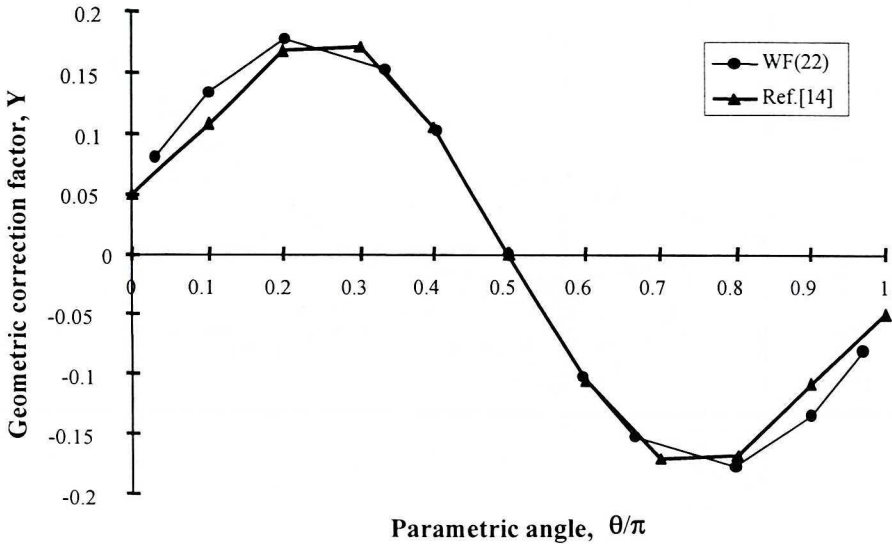

Fig. 17. (b) Comparison of the weight function based SIFs with Nilsson's [15] FE data, $[\sigma(x, y) = \sigma_0 * xy/ac, a/c = 1, a/t = 0.8]$
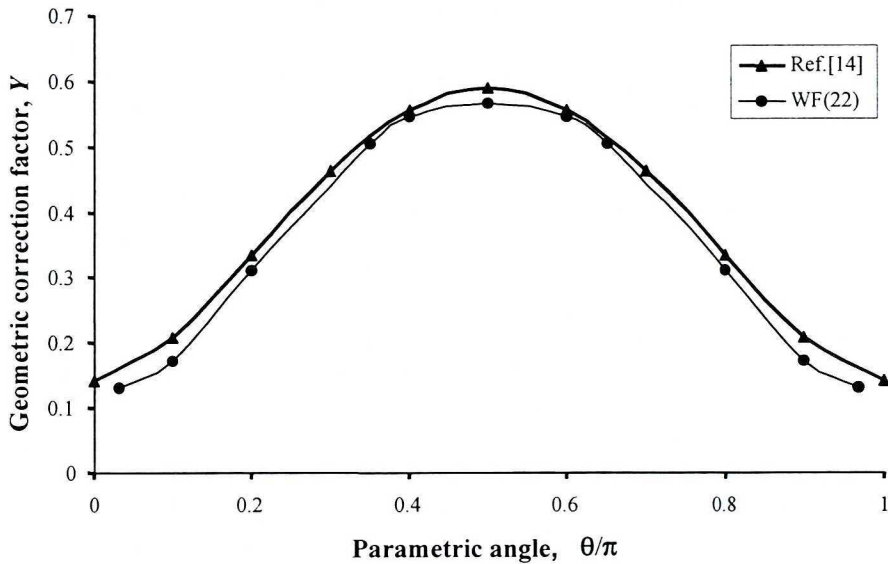
Fig. 17. (c) Comparison of the weight function based SIFs with Nilsson's [15] FE data, $[\sigma(x, y) = \sigma_0 * y/a, \ a/c = 0.5, \ a/t = 0.4]$

When the crack front approaches the free surface, the weight function based SIF deviates from the FE data of Ref. [15]. One of the reasons is that numerical integration technique was used to deal with singularities for which the integration was not sufficiently accurate. However the accuracy of integration was sufficient for the region defined by the parametric angle of $50 \le \theta \le 175^0$. The comparisons of the geometric correction factor Y obtained from the weight function (22) with the FE data of Ref. [15] are shown in Figure 17(a), (b) and (c).

For a single surface crack in a finite thickness plate, the weight function (14) yields good results for cracks with the relative depth of $a/t < 0.8$ and aspect ratio $a/c > 0.5$. Unfortunately, the weight function (22) requires an additional term accounting for the effect of bending occurring in long and deep cracks with the aspect ratio $a/c < 0.3$. Therefore further studies are being carried out in order to include the bending effect in edge cracks $(a/c \rightarrow 0)$ and semi-elliptical surface cracks with the aspect ratio of $a/c < 0.3$. The weight function (22) yields good results for embedded elliptical and other planar cracks.

5. Conclusion

The point load weight functions for edge cracks in finite bodies agree well with the finite element data obtained for the same configurations. The line

load weight functions obtained by the integration of point load weight functions also agree well with exiting literature data. There is a possibility to extend the application of the weight functions discussed above to semi-elliptical surface and corner cracks.

REFERENCES

[1] Bueckner H. F.: A Novel Principle for the Computation of stress intensity factors. Zeitschrift für Angewandte Mathematik und Mechanik, Vol. 50, 1970, pp. 529÷546.

[2] Rice J. R.: Some Remarks on Elastic Crack-Tip Stress Field, International Journal of Solids and Structures, Vol. 8, 1972, pp. 751÷758.

[3] Tada H., Paris P. and Irwin G.: The Stress Analysis of Cracks Handbook, 2nd ed., Paris Production Inc., 1985, St. Louis, Mo.

[4] Wu X. R. and Carlsson A. J.: Weight Functions and Stress Intensity Factor Solutions, 1991, Pergamon Press, Oxford, UK.

[5] Fett T. and Munz D.: Stress Intensity Factors and Weight Functions for One-Dimensional Cracks, Report No. KfK 5290, Kernforschungszentrum Karlsruhe, Institut für Materialforschung, Dezember, 1994, Karlsruhe, Germany.

[6] Molski K. L.: Method of Stress Intensity Calculation Based on the Unitary Weight Function. Journal of Theoretical and Applied Mechanics, Vol. 1, No. 32, 1994, pp. 153÷161.

[7] Glinka G. and Shen G.: Universal Features of Weight Functions for Cracks in Mode I, Engineering Fracture Mechanics, Vol. 40, No. 6, 1991, pp. 1135÷1146.

[8] Shen G. and Glinka G.: Determination of Weight Functions from Reference Stress Intensity Factors, Theoretical and Applied Fracture Mechanics, Vol. 15, No. 2, 1991, pp. 237÷245.

[9] Shen G. and Glinka G.: Weight Functions for a Surface Semi-Elliptical Crack in a Finite Thickness Plate, Theoretical and Applied Fracture Mechanics, Vol. 15, No. 2, 1991, pp. 247÷255.

[10] Zheng X. J., Glinka G. and Dubey R.: Calculation of Stress Intensity Factors for Semi-Elliptical Surface Cracks in a Thick-Wall Cylinder, International Journal of Pressure Vessels and Piping, Vol. 62, 1995, pp. 249÷258.

[11] Rice J.: Weight Function Theory for Three-Dimensional Elastic Crack Analysis, Fracture Mechanics Perspectives and Directions (20th Symposium), ASTM STP 1020, American Society for Testing and Materials, 1989, pp. 29÷57.

[12] Oore M. and Burns D. J.: Estimation of Stress Intensity Factors for Embedded Irregular Cracks Subjected to Arbitrary Normal Stress Fields, Journal of Pressure Vessel Technology, ASME, Vol. 102, 1980, pp. 201÷211.

[13] Glinka G., Reinhardt W.: Calculation of Stress Intensity Factors for Cracks of Complex Geometry and Subjected to Arbitrary Nonlinear Stress Fields. Fatigue and Fracture Mechanics, Vol. 31, ASTM STP 1389, G.R. Halford and J.P. Gallagher, Eds., American Society for Testing and Materials, West Conshohocken, PA, 2000, pp. 348÷370.

[14] Murakami Y.: Stress Intensity Factors Handbook, Vol. 2, Pergamon Press.

[15] Nilssen L.: SAQ/FoU-Report 98/10, Stress Intensity Factors for Half-Elliptical Surface Cracks in Plates Subjected to a Complex Stress Field, ISSN 1401-5331.

[16] Fett T., Mattheck C. and Munz D.: On the Calculation of Crack Opening Displacement from the Stress Intensity Factor. Engineering Fracture Mechanics, Vol. 27, No. 6, 1987.

[17] Broek D.: The Practical Use of Fracture Mechanics, Amsterdam, Kluwer, 1988.

[18] Newman J. C. and Raju I. S.: Stress Intensity Factors Equations for Cracks in Three Dimensional Bodies Subjected to Tension and Bending. in: Computational Method in the Mechanics of Fracture. S.N. Alturi, Ed., (North-Holland: Amsterdam), 1986.

[19] Shiratori M., Niyoshi T. and Tanikawa K.: Analysis of Stress Intensity Factors for Surface Cracks Subjected to Arbitrarily Distributed Surface Stress, in: Stress Intensity Factors Handbook, Y. Murakami et al., Eds., Vol. 2, (Pergamon: Oxford), 1987.

[20] Sih G. C.: in Treatise on Fracture. H. Liebowitz, Ed., Vol. II, Academic Press, New York, 1968, pp. 6.

[21] Tada H., Paris P. and Irwin G.: The Stress Analysis of Cracks Handbook, 2nd ed., Paris Production Inc., St. Louis, Mo, 1985.

Wyznaczanie współczynnika intensywności naprężeń dla szczelin w złożonych polach naprężeń

Streszczenie

Pęknięcia w elementach maszyn podlegają naprężeniom wywołanym obciążeniami zewnętrznymi oraz naprężeniom własnym wywołanym procesem technologicznym wytwarzania tych elementów. Pola naprężeń obciążających szczelinę charakteryzują się w takich przypadkach nierównomiernymi rozkładami, dla których nie istnieją wzory na współczynniki intensywności naprężeń. Przedstawiona metoda opiera się na ogólnej metodzie funkcji wagowych i umożliwia obliczanie współczynnika intensywności naprężeń dla dowolnych wypukłych szczelin płaskich przy I sposobie pękania. Metoda nadaje się w szczególności do modelowania wzrostu pęknięć zmęczeniowych przy dowolnym rozkładzie naprężeń obciążających szczelinę.

* * *

Nomenclature

a	Depth of an edge crack or the shorter semi-axis of an elliptical crack
c	The long semi-axis of an elliptical crack
A	Point on the crack contour where the stress intensity factor is to be calculated
G_c	Crack contour
G_b	External boundary contour
Ω	Crack area
K_I	Mode I stress intensity factor (general)
K_{IA}	Mode I stress intensity factor at the point A on the crack front

M_i Coefficients of the 1-D line load weight functions (i = 1,2,3)

$M(x, a)$ Weight function (general)

$M_A(x, y, F)$ Weight function for point A on the crack contour

F Point load (force) applied to the crack surface at point P (x, y)

$P(x, y)$ Point on the crack surface where the load F is applied

SIF Stress intensity factor

s Shortest distance between the point load and the crack contour

t Thickness

Γ_c Inverted crack contour

Γ_b Inverted free boundary contour

ρ Distance between the point load and the point on the crack front where the SIF is to be calculated

r_A The radius of the inside circle tangent to the ellipse at the point A where the SIF is to be calculated

R The radius of the biggest inside circle tangent to the ellipse

$\sigma(x)$ One-dimensional stress distribution

$\sigma(x, y)$ Two-dimensional stress distribution

Appendix: Examples of 1-D weight functions for cracks in plates

Central trough crack (valid for $0 < a/t < 0.9$)

$$m_1 = 0.06987 + 0.40117 \left(\frac{a}{t}\right) - 5.5407 \left(\frac{a}{t}\right)^2 + 50.0886 \left(\frac{a}{t}\right)^3$$

$$M_1 = m_1 - 200.699 \left(\frac{a}{t}\right)^4 + 395.552 \left(\frac{a}{t}\right)^5 - 377.939 \left(\frac{a}{t}\right)^6 + 140.218 \left(\frac{a}{t}\right)^7 \quad \text{(A1)}$$

$$m_2 = -0.09049 - 2.14886 \left(\frac{a}{t}\right) + 22.5325 \left(\frac{a}{t}\right)^2 - 89.6553 \left(\frac{a}{t}\right)^3$$

$$M_2 = m_2 + 210.599 \left(\frac{a}{t}\right)^4 - 239.445 \left(\frac{a}{t}\right)^5 + 111.128 \left(\frac{a}{t}\right)^6 \quad \text{(A2)}$$

$$m_3 = 0.427216 + 2.56001 \left(\frac{a}{t}\right) - 29.6349 \left(\frac{a}{t}\right)^2 + 138.4 \left(\frac{a}{t}\right)^3$$

$$M_3 = m_3 - 347.255 \left(\frac{a}{t}\right)^4 + 457.128 \left(\frac{a}{t}\right)^5 - 295.882 \left(\frac{a}{t}\right)^6 + 68.1575 \left(\frac{a}{t}\right)^7 \quad \text{(A3)}$$

Edge crack (valid for $0 < a/t < 0.9$)

$$M_1 = \frac{-0.029207 + \frac{a}{t}(0.213074 + \frac{a}{t}(-3.029553 + \frac{a}{t}(5.901933 - \frac{a}{t}2.657820)))}{1.0 + \frac{a}{t}(-1.259723 + \frac{a}{t}(-0.048475 + \frac{a}{t}(0.481250 + \frac{a}{t}(-0.526796 + \frac{a}{t}0.345012))))} \qquad (A4)$$

$$M_2 = \frac{0.451116 + \frac{a}{t}(3.462425 + \frac{a}{t}(-1.078459 + \frac{a}{t}(3.558573 - \frac{a}{t}7.553533)))}{1.0 + \frac{a}{t}(-1.496612 + \frac{a}{t}(0.764586 + \frac{a}{t}(-0.659316 + \frac{a}{t}(0.258506 + \frac{a}{t}0.114568))))} \qquad (A5)$$

$$M_3 = \frac{0.427195 + \frac{a}{t}(-3.730114 + \frac{a}{t}(16.276333 + \frac{a}{t}(-18.799956 + \frac{a}{t}14.112118)))}{1.0 + \frac{a}{t}(-1.129189 + \frac{a}{t}(0.033758 + \frac{a}{t}(0.192114 + \frac{a}{t}(-0.658242 + \frac{a}{t}0.554666))))} \qquad (A6)$$

Surface semi-elliptical crack (valid for $0 < a/t < 0.8$)
- **the deepest point A**

$$M_{1A} = \frac{\pi}{\sqrt{2Q}}(4Y_0 - 6Y_1) - \frac{24}{5} \qquad (A7)$$

$$M_{2A} = 3 \qquad (A8)$$

$$M_{3A} = 2\left(\frac{\pi}{\sqrt{2Q}}Y_0 - M_{1A} - 4\right) \qquad (A9)$$

where for $0 < a/c < 1$:

$$Q = 1.0 + 1.464\left(\frac{a}{c}\right)^{1.65} \qquad (A10)$$

$$Y_0 = B_0 + B_1\left(\frac{a}{t}\right)^2 + B_2\left(\frac{a}{t}\right)^4 + B_3\left(\frac{a}{t}\right)^6 \qquad (A11)$$

$$B_0 = 1.0929 + 0.2581\left(\frac{a}{c}\right) - 0.7703\left(\frac{a}{c}\right)^2 + 0.4394\left(\frac{a}{c}\right)^3 \qquad (A12)$$

$$B_1 = 0.456 - 3.045\left(\frac{a}{c}\right) + 2.007\left(\frac{a}{c}\right)^2 + \frac{1.0}{0.147 + \left(\frac{a}{c}\right)^{0.688}} \qquad (A13)$$

$$B_2 = 0.995 - \frac{1.0}{0.027 + \dfrac{a}{c}} + 22.0 \left(1 - \frac{a}{c} \right)^{9.953} \tag{A14}$$

$$B_3 = -1.459 + \frac{1.0}{0.014 + \dfrac{a}{c}} - 24.211 \left(1 - \frac{a}{c} \right)^{8.071} \tag{A15}$$

and

$$Y_1 = A_0 + A_1 \left(\frac{a}{t} \right)^2 + A_2 \left(\frac{a}{t} \right)^4 + A_3 \left(\frac{a}{t} \right)^6 \tag{A16}$$

$$A_0 = 0.4537 + 0.1231 \left(\frac{a}{c} \right) - 0.7412 \left(\frac{a}{c} \right)^2 + 0.4600 \left(\frac{a}{c} \right)^3 \tag{A17}$$

$$A_1 = -1.652 + 1.665 \left(\frac{a}{c} \right) - 0.534 \left(\frac{a}{c} \right)^2 + \frac{1.0}{0.198 + \left(\dfrac{a}{c} \right)^{0.846}} \tag{A18}$$

$$A_2 = 3.418 - 3.126 \left(\frac{a}{c} \right) - \frac{1.0}{0.041 + \left(\dfrac{a}{c} \right)} + 17.259 \left(1 - \frac{a}{c} \right)^{9.286} \tag{A19}$$

$$A_3 = -4.228 + 3.643 \left(\frac{a}{c} \right) + \frac{1.0}{0.020 + \dfrac{a}{c}} - 21.924 \left(1 - \frac{a}{c} \right)^{9.203} \tag{A20}$$

and for $1 < a/c < 2$

$$Q = 1.0 + 1.464 \left(\frac{c}{a} \right)^{1.65} \left(\frac{a}{c} \right)^2 \tag{A21}$$

$$Y_0 = B_0 + B_1 \left(\frac{a}{t} \right)^2 + B_2 \left(\frac{a}{t} \right)^4 \tag{A22}$$

$$B_0 = 1.12 - 0.09923 \left(\frac{a}{c} \right) + 0.02954 \left(\frac{a}{c} \right)^2 \tag{A23}$$

$$B_1 = 1.138 - 1.134 \left(\frac{a}{c}\right) + 0.3073 \left(\frac{a}{c}\right)^2 \tag{A24}$$

$$B_2 = -0.9502 + 0.8832 \left(\frac{a}{c}\right) - 0.2259 \left(\frac{a}{c}\right)^2 \tag{A25}$$

$$Y_1 = A_0 + A_1 \left(\frac{a}{t}\right)^2 + A_2 \left(\frac{a}{t}\right)^4 \tag{A26}$$

$$A_0 = 0.4735 - 0.2053 \left(\frac{a}{c}\right) + 0.03662 \left(\frac{a}{c}\right)^2 \tag{A27}$$

$$A_1 = 0.7723 - 0.7265 \left(\frac{a}{c}\right) + 0.1837 \left(\frac{a}{c}\right)^2 \tag{A28}$$

$$A_2 = -0.2006 - 0.9829 \left(\frac{a}{c}\right) + 1.237 \left(\frac{a}{c}\right)^2 - 0.3554 \left(\frac{a}{c}\right)^3 \tag{A29}$$

- **the surface point B**

$$M_{1B} = \frac{\pi}{\sqrt{4Q}} (30F_1 - 18F_0) - 8 \tag{A30}$$

$$M_{2B} = \frac{\pi}{\sqrt{4Q}} (60F_0 - 90F_1) + 15 \tag{A31}$$

$$M_{3B} = -(1 + M_{1B} + M_{1B}) \tag{A32}$$

where for $0 < a/c < 1$:

$$F_0 = \left[C_0 + C_1 \left(\frac{a}{t}\right)^2 + C_2 \left(\frac{a}{t}\right)^4 \right] \sqrt{\frac{a}{c}} \tag{A33}$$

$$C_0 = 1.2972 - 0.1548 \left(\frac{a}{c}\right) - 0.0185 \left(\frac{a}{c}\right)^2 \tag{A34}$$

$$C_1 = 1.5083 - 1.3219 \left(\frac{a}{c}\right) + 0.5128 \left(\frac{a}{c}\right)^2 \tag{A35}$$

$$C_2 = -1.101 + \frac{0.879}{0.157 + \dfrac{a}{c}} \tag{A36}$$

and

$$F_1 = \left[D_0 + D_1 \left(\frac{a}{t} \right)^2 + D_2 \left(\frac{a}{t} \right)^4 \right] \sqrt{\frac{a}{c}} \tag{A37}$$

$$D_0 = 1.2687 - 1.0642 \left(\frac{a}{c} \right) + 1.4646 \left(\frac{a}{c} \right)^2 - 0.7250 \left(\frac{a}{c} \right)^3 \tag{A38}$$

$$D_1 = 1.1207 - 1.2289 \left(\frac{a}{c} \right) + 0.5876 \left(\frac{a}{c} \right)^2 \tag{A39}$$

$$D_2 = 0.190 - 0.608 \left(\frac{a}{c} \right) + \frac{0.199}{0.035 + \dfrac{a}{c}} \tag{A40}$$

and for $1 < a/c < 2$

$$F_0 = \left[C_0 + C_1 \left(\frac{a}{t} \right)^2 + C_2 \left(\frac{a}{t} \right)^4 \right] \sqrt{\frac{a}{c}} \tag{A41}$$

$$C_0 = 1.34 - 0.2872 \left(\frac{a}{c} \right) + 0.0661 \left(\frac{a}{c} \right)^2 \tag{A42}$$

$$C_1 = 1.882 - 1.7569 \left(\frac{a}{c} \right) + 0.4423 \left(\frac{a}{c} \right)^2 \tag{A43}$$

$$C_2 = -0.1493 + 0.01208 \left(\frac{a}{c} \right) + 0.02215 \left(\frac{a}{c} \right)^2 \tag{A44}$$

and

$$F_1 = \left[D_0 + D_1 \left(\frac{a}{t} \right)^2 + D_2 \left(\frac{a}{t} \right)^4 \right] \sqrt{\frac{a}{c}} \tag{A45}$$

$$D_0 = 1.12 - 0.2442 \left(\frac{a}{c} \right) + 0.06708 \left(\frac{a}{c} \right)^2 \tag{A46}$$

$$D_1 = 1.251 - 1.173 \left(\frac{a}{c} \right) + 0.2973 \left(\frac{a}{c} \right)^2 \tag{A47}$$

$$D_2 = 0.04706 - 0.1214 \left(\frac{a}{c} \right) + 0.04406 \left(\frac{a}{c} \right)^2 \tag{A48}$$